Supplementary Information

Seeding Approach to Noble Metal Decorated Conducting Polymer Nanofiber Network

Zhen Liu, Selcuk Poyraz, Yang Liu, Xinyu Zhang*

Department of Polymer and Fiber Engineering, Auburn University, Auburn, AL 36849

Synthesis of polypyrrole (PPy) and noble metal nanocomposites

In a typical synthesis, 1-2 mg of V_2O_5 sol-gel nanofibers were slowly added into the noble metal salt solutions under magnetic stirring. After the addition of V_2O_5, 0.1mL of pyrrole monomer was added to the reaction media in a 60-second period. The solution color was spontaneously darkened and turned into black with the formation and dispersion of black precipitates of PPy. The reaction solution was magnetically stirred for 24 hours for the completion of polymerization and a better homogenous noble metal nanoparticles distribution into PPy nanofibers. The resulting black precipitate of polypyrrole was suction filtered, washed with copious amounts of aq. 1M HCl (3×100mL) and acetone (3×100mL) and freeze dried for 12h. The yield of nanocomposites powder was ~50-100 mg depending on different types of metal salts.

TEM sample preparation of PPy Nanofiber-Nobel Metal Nanoparticle Composites (PNNMN)

In a typical process, 5 mg of the as-synthesized PNNMN composite was weighted and dispersed in 10 mL ethanol with bath sonication for 20 minutes. The resultant dispersion was drop casted onto the copper grid and dried for TEM characterization.

Potential-time profiling characterization of in-situ polymerization process

The reaction mixture was characterized by potential-time profiling using established methods,[1-3] (Pt wire electrode, saturated calomel electrode (SCE) reference). The electrode configuration was immersed into the reaction solution before starting the polymerization reaction. Each reactant required for the polymerization process was added following the sequence of metal salts, V_2O_5, and finally pyrrole monomer. 10 minutes' interval was allowed between the addition of each reactant, which would give better indication about the potential change according to the potential-time profiling curve. The potential of the reaction solution was monitored and recorded from the beginning of each individual polymerization experiment and the corresponding control experiment without the addition of V_2O_5 nanofibers.

Electrochemical tests for PPy-Pt and PPy-Au catalysts

The electrochemical behaviors of PPy-Pt and PPy-Au catalysts were measured by Cyclic Voltammetry (CV) at room temperature in a three-electrode cell using Arbin electrochemical instrument (Arbin-010 MITS Pro 4-BT 2000). Bare graphite rod was used as counter electrode; PPy (control), PPy-noble metal nanocomposites (1-2 mg) and nanocarbon-noble metal nanocomposites (1-2 mg) were uniformly decorated on the tip of the graphite rod electrode with carbon colloids paste to fabricate three types of working electrode, respectively. Saturated Calomel Electrode (SCE) was used as the reference electrode. Tests were conducted by cycling the potential between -0.8V to 0.4V vs. SCE in 1M aq. KOH solution, 5 vol.% of CH_3OH. The scan rate was set at 20mV/s.

The discharge capacity of the PPy-Pt catalysts was measured by modifying the graphite electrode with these catalysts and subjecting the modified electrode to CV test in the same three-electrode cell configuration. Pt wire was used as the counter electrode and Ag/AgCl electrode was used as the reference. The CV characteristic of the modified electrode was measured in 1M KCl solution with a cyclic range of -0.8V-0.8V at a scan rate of 50 mV/s. The discharge capacity of the PPy-Pt catalysts was measured simultaneously as the CV characteristic of the modified electrode was recorded.

Microwave synthesis of Nanocarbon-Noble Metal Nanoparticle (NCNMN) composites from PPy Nanofiber-Noble Metal Nanoparticle (PNNMN) composites

50 mg of the as-synthesized nanocomposite material were placed in a glass vial and then irradiated in a conventional microwave oven, under ambient condition for 5-6 min. Sparks were observed at nanocomposite surfaces during microwave heating. It is found from the field emission scanning electronic microscopy (FE-SEM) that the morphology of NCNMN is consistent with its microwave precursor PNNMN (Figures S7 and S8).

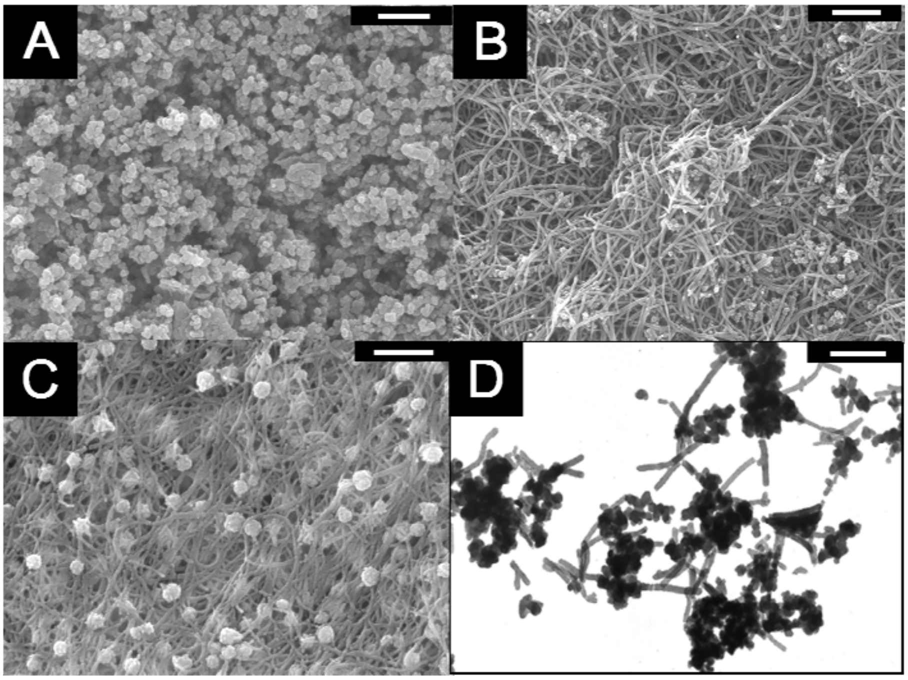

Figure S1. SEM images: (A) PPy granules oxidized by $PtCl_2$ without V_2O_5 seeds; (B) PPy/Au nanofiber composites from V_2O_5/pyrrole/AuCl system; (C) PPy/Pt nanofiber composites from V_2O_5/pyrrole/$PtCl_4$ system; and (D) TEM image of PPy/Pt nanofiber composites from V_2O_5/pyrrole/$PtCl_4$, scale bar: 500 nm.

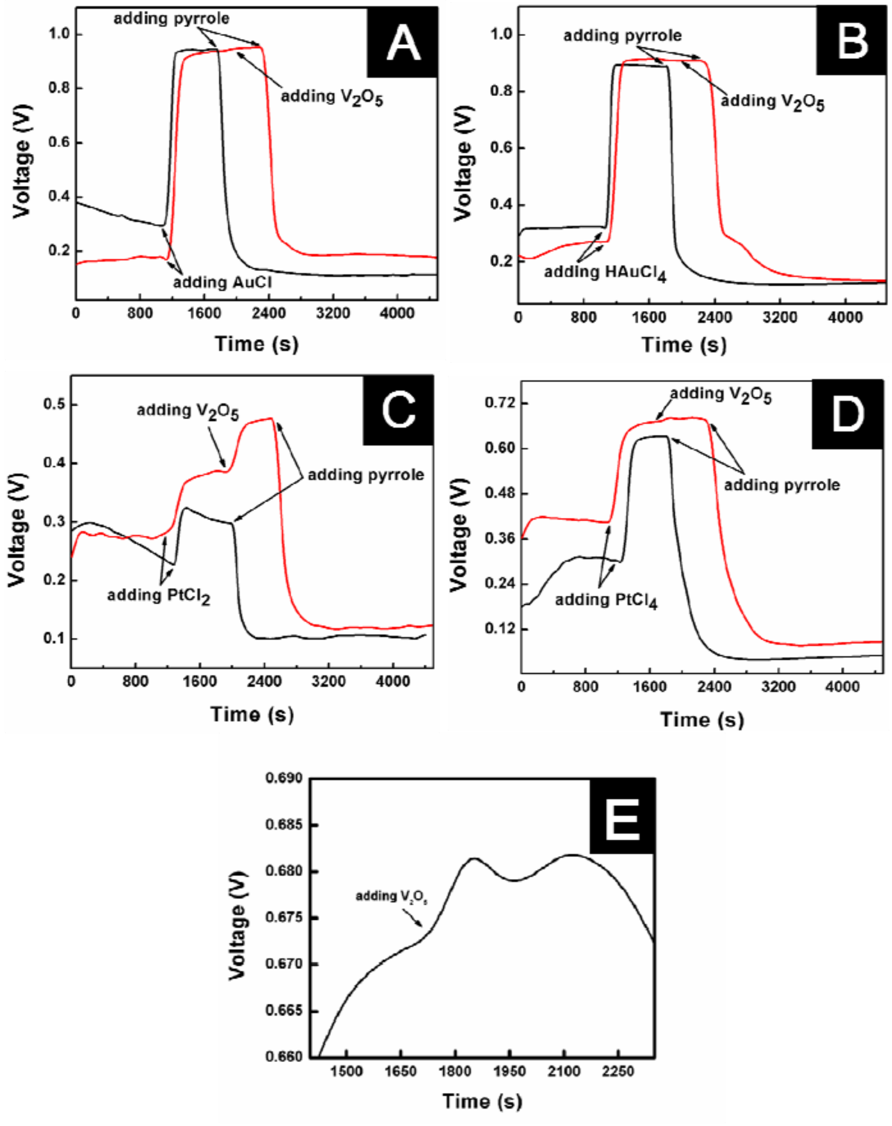

Figure S2. Potential-time profiles of pyrrole polymerization via different systems between seeding and non-seeding approach: (A) V_2O_5/pyrrole/AuCl; (B) V_2O_5/pyrrole/$HAuCl_4$; (C) V_2O_5/pyrrole/ $PtCl_2$; and (D) V_2O_5/pyrrole/$PtCl_4$; (E) a zoom-in view of oxidation potential increment by adding V_2O_5 to pyrrole/$PtCl_4$ system

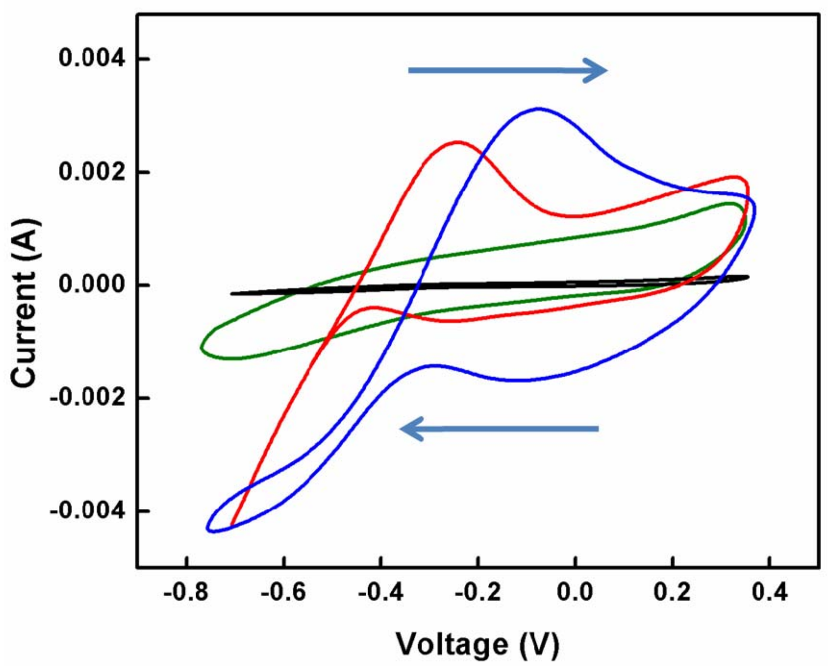

Figure S3. Cyclic voltammograms: Black: bare graphite electrode; Green: PPy nanofiber on graphite electrode; Blue: PPy nanofiber-Pt nanoparticles on graphite electrode; Red: microwave heated PPy nanofiber-Pt nanoparticles on graphite electrode.

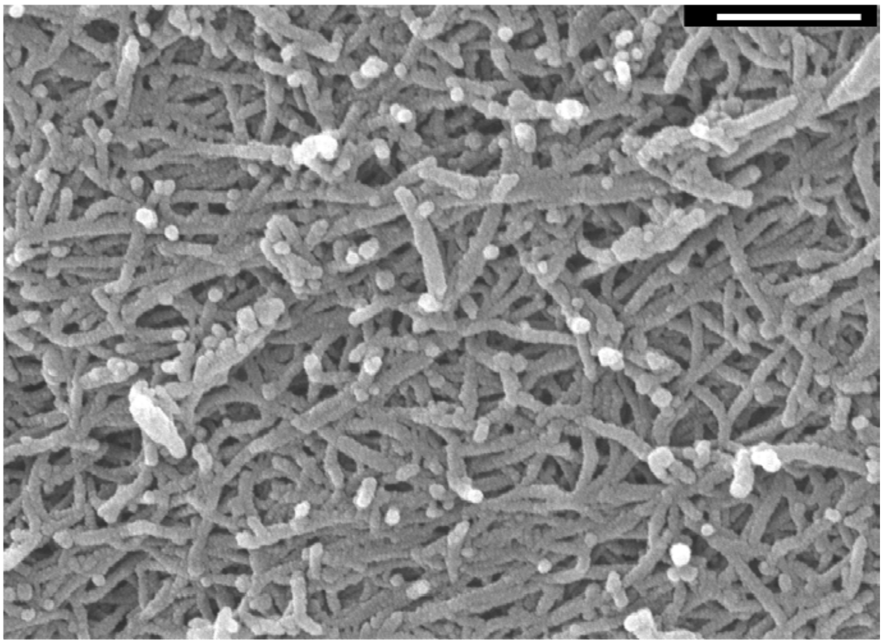

Figure S4. SEM image: PPy/Ag nanofiber composites from V_2O_5/pyrrole/$AgNO_3$ system, scale bar: 1 μm

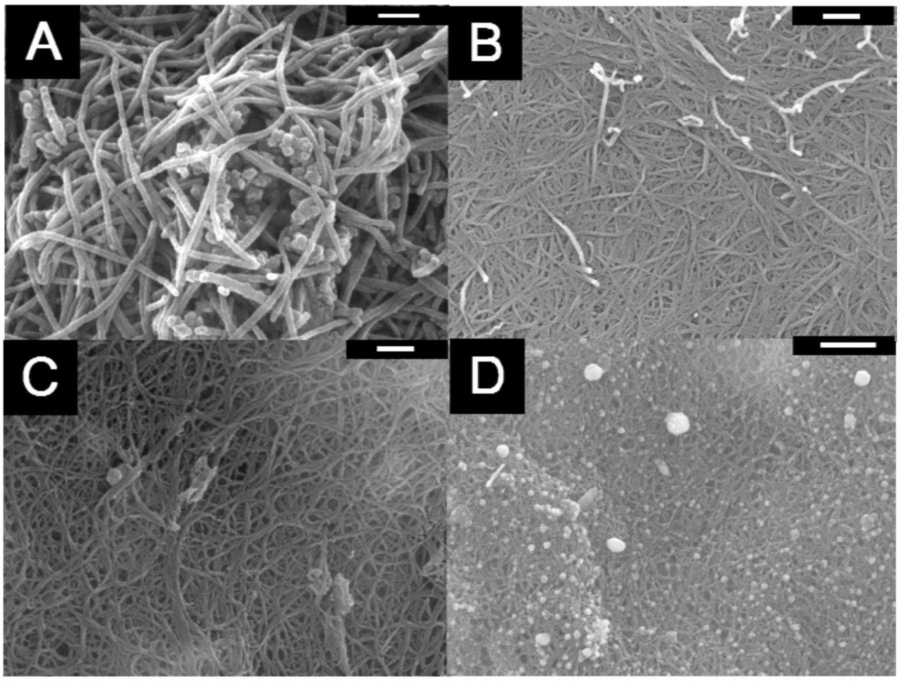

Figure S5. Polypyrrole-noble metal nanofiber composites (before and after microwave) SEM images from: (a) V_2O_5/pyrrole/AuCl system before microwave; (b) V_2O_5/pyrrole/AuCl system after microwave; (c) V_2O_5/pyrrole/$HAuCl_4$ system before microwave; and (d) V_2O_5/pyrrole/$HAuCl_4$ system after microwave, scale bar: 500 nm.

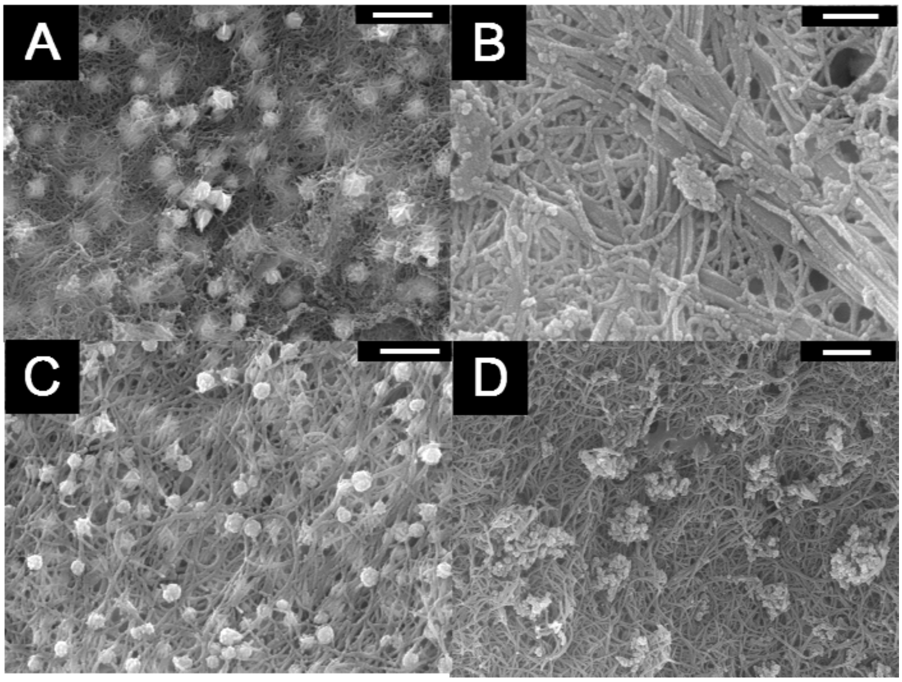

Figure S6. Polypyrrole-noble metal nanofiber composites (before and after microwave) SEM images from: (a) V_2O_5/pyrrole/$PtCl_2$ system before microwave; (b) V_2O_5/pyrrole/$PtCl_2$ system after microwave; (c) V_2O_5/pyrrole/$PtCl_2$ system before microwave; and (d) V_2O_5/pyrrole/$PtCl_2$ system after microwave, scale bar: 500 nm.

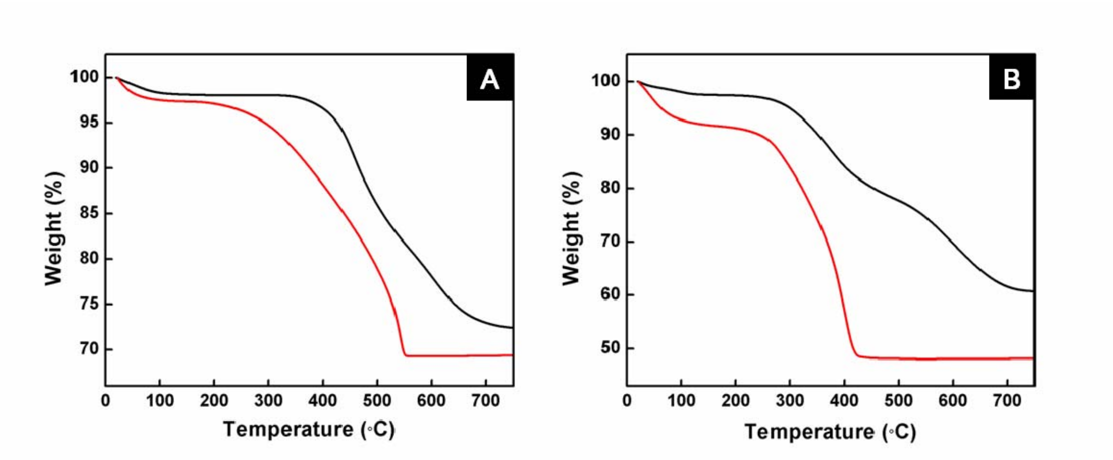

Figure S7. Thermogravimetric Analysis (TGA) of (A) PPy-Au nanofiber composites (V_2O_5/pyrrole/AuCl system) before (red) and after (black) microwave heating and (B) PPy-Pt nanofiber composites (V_2O_5/pyrrole/$PtCl_4$ system) before (red) and after (black) microwave heating. Heating rate: 10°C/min, under N_2 flow.

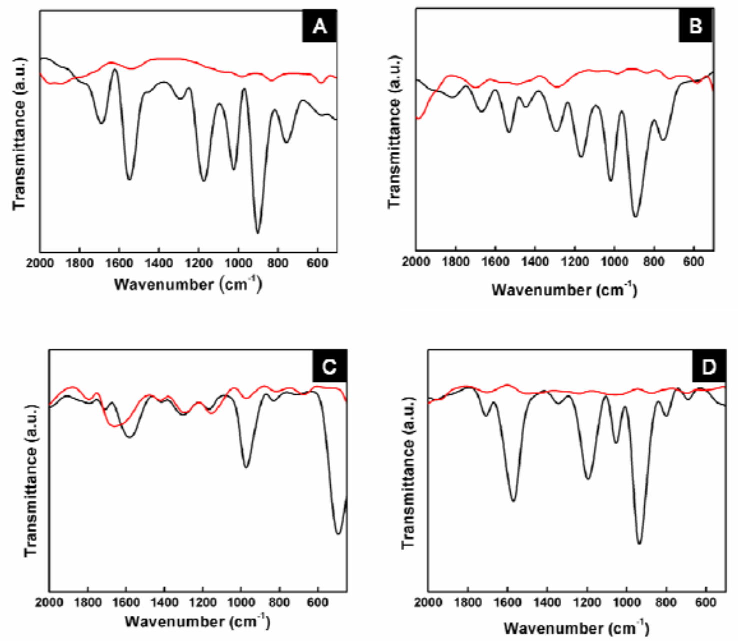

Figure S8. FTIR of (A) PPy-Au nanocomposites from V_2O_5/pyrrole/AuCl system, before (black) and after (red) microwave heating; (B) PPy-Au nanocomposites from V_2O_5/pyrrole/$HAuCl_4$ system before (black) and after (red) microwave heating; (C) PPy-Pt nanocomposites from V_2O_5/pyrrole/$PtCl_2$ system before (black) and after (red) microwave heating; (D) PPy-Pt nanocomposites from V_2O_5/pyrrole/$PtCl_4$ system before (black) and after (red) microwave heating

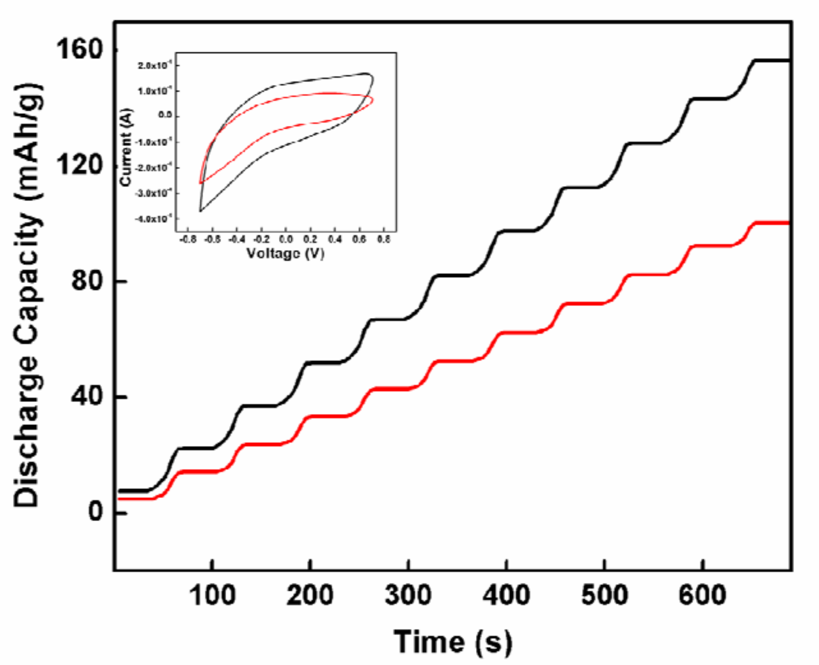

Figure S9. Discharge capacity plot of PPy-Pt nanofiber composites before (red) and after (black) microwave heating in the range of -0.8-0.8V (vs. Ag/AgCl) in aqueous 1.0 M KCl electrolyte. Inset: cyclic voltammograms of PPy-Pt nanofiber composite before (red) and after (black) microwave in the range of -0.8-0.8V (vs. Ag/AgCl) in aqueous 1.0 M KCl electrolyte.

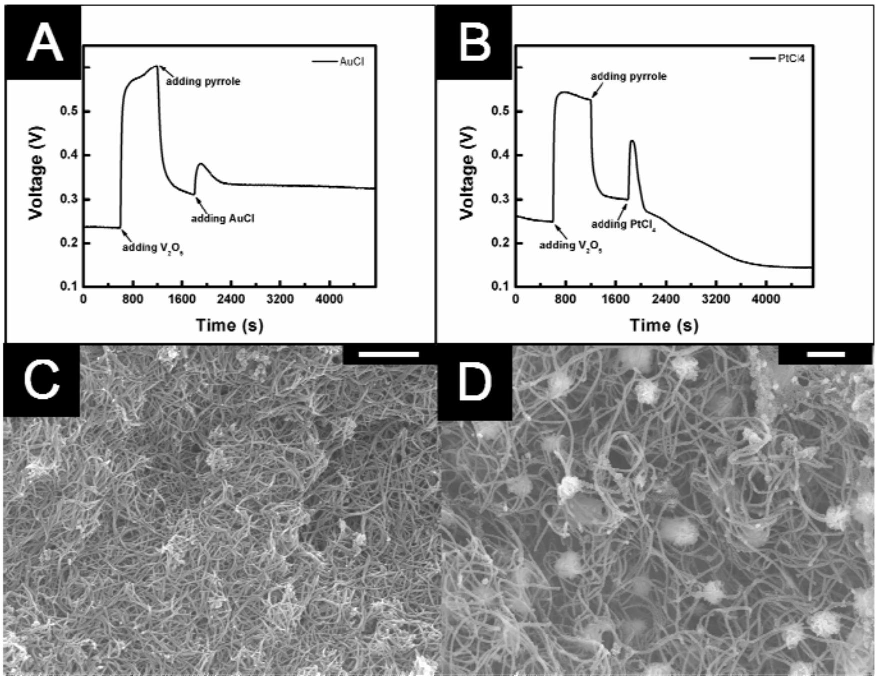

Figure S10. Potential-time profiles of pyrrole polymerization via different reagent addition sequences: (a) V_2O_5/pyrrole/AuCl sequence; (b) V_2O_5/pyrrole/$PtCl_4$ sequence; Polypyrrole-noble metal nanofiber composites SEM images from: (c) V_2O_5/pyrrole/AuCl system; (d) V_2O_5/pyrrole/$PtCl_4$ system. Scale bar: 500 nm

Table S1: EDX data of the nanocomposites made in different systems

Systems	C	N	O	Cl	V	Au / Pt	Total
V_2O_5/Pyrrole/AuCl 0.005M	34.98	9.93	4.96	0.69	-0.10	49.54	100
V_2O_5/Pyrrole/AuCl 0.01M	36.59	9.17	5.44	0.97	-0.17	47.99	100
V_2O_5/Pyrrole/AuCl 0.02M	30.26	8.69	4.03	1.80	0.07	55.14	100
V_2O_5/Pyrrole/$HAuCl_4$ 0.005M	43.42	14.50	5.08	2.00	0.16	34.83	100
V_2O_5/Pyrrole/$HAuCl_4$ 0.01M	39.26	10.09	2.89	2.35	0.24	45.17	100
V_2O_5/Pyrrole/$HAuCl_4$ 0.02M	43.45	9.05	4.92	4.48	-0.02	38.14	100
V_2O_5/Pyrrole/$PtCl_2$ 0.005M	32.44	6.73	10.78	8.61	6.22	35.21	100
V_2O_5/Pyrrole/$PtCl_2$ 0.01M	29.42	5.91	9.10	11.07	2.75	41.76	100
V_2O_5/Pyrrole/$PtCl_2$ 0.02M	27.79	4.96	5.28	12.86	0.93	48.18	100
V_2O_5/Pyrrole/$PtCl_4$ 0.005M	34.39	6.37	7.19	9.37	0.18	42.50	100
V_2O_5/Pyrrole/$PtCl_4$ 0.01M	38.24	5.38	5.45	9.06	0.20	41.68	100
V_2O_5/Pyrrole/$PtCl_4$ 0.02M	33.34	9.16	5.31	9.99	0.20	41.99	100

(1) Manohar, S. K.; Macdiarmid, A. G.; Epstein, A. J. *Synthetic Metals* **1991**, *41*, 711-714.
(2) Wei, Y.; Hsueh, K. F.; Jang, G. W. *Polymer* **1994**, *35*, 3572-3575.
(3) Mattoso, L. H. C.; Oliveira, O. N.; Faria, R. M.; Manohar, S. K.; Epstein, A. J.; Macdiarmid, A. G. *Polymer International* **1994**, *35*, 89-93.